Original Article

MOLECULAR METABOLISM

# Suppression of hepatic ChREBPα-CYP2C50 axis-driven fatty acid oxidation sensitizes mice to diet-induced MASLD/MASH

**Deqiang Zhang[1,2,8], Yuee Zhao[1,2,3,8], Gary Zhang[1,2], Daniel Lank[4], Sarah Cooke[5], Sujuan Wang[6], Alli Nuotio-Antar[7], Xin Tong[1,2,9], Lei Yin[1,2,*,9]**

## ABSTRACT

**Objectives:** Compromised hepatic fatty acid oxidation (**FAO**) has been observed in human MASH patients and animal models of MASLD/MASH. It remains poorly understood how and when the hepatic FAO pathway is suppressed during the progression of MASLD towards MASH. Hepatic ChREBPα is a classical lipogenic transcription factor that responds to the intake of dietary sugars.

**Methods:** We examined its role in regulating hepatocyte fatty acid oxidation (FAO) and the impact of hepatic *Chrebpa* deficiency on sensitivity to diet-induced MASLD/MASH in mice.

**Results:** We discovered that hepatocyte ChREBPα is both necessary and sufficient to maintain FAO in a cell-autonomous manner independently of its DNA-binding activity. Supplementation of synthetic PPARα/δ agonist is sufficient to restore FAO in *Chrebp*$^{-/-}$ primary mouse hepatocytes. Hepatic ChREBPα was decreased in mouse models of diet-induced MAFSLD/MASH and in patients with MASH. Hepatocyte-specific *Chrebpα* knockout impaired FAO, aggravated liver steatosis and inflammation, leading to early-onset fibrosis in response to diet-induced MASH. Conversely, liver overexpression of ChREBPα-WT or its non-lipogenic mutant enhanced FAO, reduced lipid deposition, and alleviated liver injury, inflammation, and fibrosis. RNA-seq analysis identified the CYP450 epoxygenase (CYP2C50) pathway of arachidonic acid metabolism as a novel target of ChREBPα. Over-expression of CYP2C50 partially restores hepatic FAO in primary hepatocytes with *Chrebpα* deficiency and attenuates preexisting MASH in the livers of hepatocyte-specific *Chrebpα*-deleted mice.

**Conclusions:** Our findings support the protective role of hepatocyte ChREBPa against diet-induced MASLD/MASH in mouse models in part via promoting CYP2C50-driven FAO.

© 2024 The Authors. Published by Elsevier GmbH. This is an open access article under the CC BY-NC-ND license (http://creativecommons.org/licenses/by-nc-nd/4.0/).

**Keywords** Lipid metabolism; Fatty acid oxidation; Metabolic-Associated Steatohepatitis; Carbohydrate-response element binding protein (ChREBP)

## 1. INTRODUCTION

Hepatic lipid metabolic homeostasis is maintained by coordinated regulation of *de novo* lipogenesis (DNL), fatty acid oxidation (FAO), lipid uptake, and lipoprotein secretion during normal fasting and feeding cycles [1—4]. Mounting evidence to date has highlighted that the disruption of hepatic lipid homeostasis is persistent during both the onset and progression of MASLD [3,4]. Animal models and human patients with MASLD have shown that DNL and fatty acid uptake are significantly increased [5—9], while hepatic FAO is suppressed [9—12], leading to an imbalance between lipid anabolism and catabolism. Polymorphisms in several lipid metabolic genes (for example, *PNPLA3, MBOAT7,* and *TM6SF2*) were reported to be associated with an increased risk of MASLD in humans, highlighting a critical role of impaired lipid homeostasis during the pathogenesis of MASLD [13—15].

Hepatocytes utilize FAO to break down lipids as an energy source when the circulating glucose concentration is low [1,2]. This process mainly occurs within the mitochondria when acyl-fatty acids are transported via carnitine palmitoyl-transferase 1 (CPT1) [16]. Animal experiments demonstrate that the enhancement of mitochondria-mediated FAO is beneficial in treating MASLD. For example, overexpression of a permanently active mutant form of human CPT1A enhances hepatic FAO and autophagy, reduces liver steatosis, and improves glucose

[1]Department of Molecular & Integrative Physiology, USA [2]Caswell Diabetes Institute, University of Michigan Medical School, NCRC Building 20-3843, 2800 Plymouth Road, Ann Arbor, MI 48105, USA [3]Department of Nephrology, Hunan Key Laboratory of Kidney Disease and Blood Purification, The Second Xiangya Hospital, Central South University, 139 Renmin Middle Rd, Furong District, Changsha, Hunan Province 410011, PR China [4]Department of Pharmacology, University of Virginia, 1340 Jefferson Park Avenue, Charlottesville, VA 22908, USA [5]Neurosciences Graduate Program, Case Western Reserve University School of Medicine, Cleveland, OH 44016, USA [6]Department of Infectious Diseases, The Second Xiangya Hospital, Central South University, 139 Renmin Middle Rd, Furong District, Changsha, Hunan Province 410011, PR China [7]Children Nutrition Research Center, Department of Pediatrics, Baylor College of Medicine, Houston, TX 77030, USA

[8] Deqiang Zhang and Yuee Zhao contributed equally to this work.
[9] Co-corresponding authors.

*Corresponding author. Department of Molecular & Integrative Physiology, USA. E-mail: leiyin@umich.edu (L. Yin).

Received March 9, 2024 • Revision received May 3, 2024 • Accepted May 9, 2024 • Available online 11 May 2024

https://doi.org/10.1016/j.molmet.2024.101957

 © 2024 The Authors. Published by Elsevier GmbH. This is an open access article under the CC BY-NC-ND license (http://creativecommons.org/licenses/by-nc-nd/4.0/).

homeostasis [17]. Pharmacological ACC inhibitors increase CPT1a activity and hepatocyte FAO by reducing malonyl-CoA, leading to improved liver steatosis [18,19]. These findings suggest the potential therapeutic value of improving mitochondrial FAO against MASLD.

The nuclear receptor PPARα acts as the major transcription factor to activate hepatic FAO in response to energy demands or pharmacological agonists [6,20]. During the progression of MASLD, FAO and the activity of PPARα are suppressed in the liver [21]. Hepatocyte-specific *Pparα* deletion impairs fatty acid catabolism, resulting in hepatic lipid accumulation during fasting and methionine and choline-deficient (MCD) diet feeding [21,22]. Conversely, synthetic PPARα agonists have been explored extensively to treat simple liver steatosis and MASH [23,24]. In particular, phase III clinical trial of the dual PPARα/δ agonist Elafibranor has shown promise that activating the FAO pathway may be an effective approach to reducing liver steatosis, inflammation, and slowing down fibrosis in MASH patients [25]. How exactly the hepatic PPARα-driven FAO pathway is suppressed during MASH remains largely unclear. The transcriptional activity of PPARα depends on not only the expression of PPARα, RXR, and coactivators but also the levels of endogenous ligands within hepatocytes [6,20,26]. Several fatty acids and eicosanoids have been identified as endogenous ligands of PPARα, especially lipid mediators synthesized from arachidonic acid [27—29]. For example, 20-COOH-AA and 20-HETE, an eicosanoid produced from arachidonic acid by cytochrome P450 (CYP) omega-oxidases potently activate PPARα in transfected COS-7 cells [29,30]. Interestingly, the product of CYP450 epoxygenase, was found to reduce hepatic inflammation and protect mice from MCD diet-induced NASH. It has been reported that the expression of liver CYP epoxygenases (*Cyp2c50, Cyp2c54,* and *Cyp2c49*) was markedly reduced in the liver of MCD diet-fed mice [31]. A recent study showed that total epoxygenases were reduced in simple steatosis and progressively depleted with the severity of MASH [32]. Thus far, whether and how the reduction of CYP450 epoxygenase contributes to the suppression of endogenous ligands for PPARα pathway, and subsequent impairment of FAO during diet-induced MASLD/MASH has not been well examined.

Here we report that hepatocyte ChREBPα is both necessary and sufficient to activate the FAO pathway in a cell-autonomous manner. More importantly, this action is independent of its DNA binding and lipogenic activity. Liver ChREBP levels are reduced in MASH in both mice and humans. Hepatocyte-specific *Chrebp* knockout sensitizes mice to early-onset and more severe MASH, whereas hepatic overexpression of ChREBP reduces liver MASH and improves liver health. Consistent with *in vitro* findings, loss of ChREBPα reduces liver FAO, while overexpression of ChREBPα (both WT and DNA-binding deficient AG mutant) does the opposite in mouse models of diet-induced MASH. Mechanically, ChREBPα likely promotes FAO by controlling the biogenesis of endogenous ligands of PPARα via the CYP450 epoxygenase CYP2C50, one of the key players in arachidonic acid metabolism. Restoring hepatic CYP2C50 expression in the background of *Chrebpα* deficiency is sufficient to reduce liver steatosis, fibrosis, and hepatocyte injury. In summary, we provided evidence supporting the protective role of ChREBPα-CYP2C50 axis in diet-induced MASLD/MASH via its cell-autonomous action promoting hepatic FAO. Our findings also link ChREBPα non-lipogenic actions and arachidonic acid metabolism for the first time.

## 2. RESULTS

### 2.1. ChREBPα is both required and necessary for FAO in hepatocytes

The canonical action of ChREBP in hepatocytes is to sense glucose or fructose and stimulate lipogenesis [33,34]. This action requires ChREBP to form a complex with MLX, binding to its cis-elements, and activating the transcription of lipogenic enzymes [34,35]. Whether ChREBP is also required for fatty acid oxidation in a cell-autonomous manner remains untested even though a previous report suggests this possibility [36]. To examine this issue, we isolated primary hepatocytes from WT and *Chrebp*$^{-/-}$ mice and analyzed the FAO pathway. Consistent with the literature [33,37], the mRNA levels of classical DNL genes including *Acc1, Fasn and Scd1* were greatly reduced in the *Chrebp*$^{-/-}$ primary mouse hepatocytes (PMHs) (Supplementary Fig. 1A). Within the same samples, several FAO key genes [1] were markedly downregulated in *Chrebp*$^{-/-}$ hepatocytes (mRNA of *Ehhadh, Acox1,* and *Cyp4a10* and protein of ACADL and ACADM) (Figure 1A—B). Consistent with reduced expression of FAO enzymes, the rate of FAO of PMHs was significantly reduced after incubation in medium containing $H^3$-labeled palmitate (Figure 1C). Furthermore, both BODIPY staining and cellular triglyceride assay showed elevated cellular lipid accumulation in *Chrebp*$^{-/-}$ PMHs (Figure 1D—E). We also found similar responses on FAO gene expression in HUH7 human liver cancer cells following acute depletion of *Chrebpα* (Supplementary Fig. 1C).

To test if ChREBP is sufficient to drive FAO within hepatocytes, we transduced WT PMHs with Ad-Chrebpα-WT *vs.* Ad-GFP. When overexpressed in PMHs, ChREBPα promoted the mRNA levels of DNL enzymes including *Acc1* and *Fasn* (Supplementary Fig. 1B), while elevating the mRNA and protein expression of FAO enzymes (Figure 1F—G). In addition, palmitate plus oleate-induced lipid droplet formation (Figure 1H) was significantly repressed by Ad-Chrebpα *vs.* Ad-LacZ in PMHs. Moreover, the application of Etomoxir [16,38], a specific inhibitor of CPT1A, restored lipid accumulation in hepatocytes transduced with Ad-ChREBPα (Supplementary Fig. 2). Altogether, these results suggest that ChREBPα can promote the hepatocyte CPT1A-FAO pathway in a cell-autonomous manner.

SREBP-1c is another potent lipogenic transcription factor that mediates the insulin's action on DNL following food intake [39—41]. To test whether SREBP-1c has a similar function as ChREBPα in the regulation of FAO in hepatocytes, we transduced Hepa1c1c-7 cells with Ad-shSrebp-1c *vs.* Ad-shLacZ. Despite a clear reduction of the DNL genes including *Acc1* and *Scd1*, the FAO genes (*Cpt1a, Acox1, Cyp4a10, and Cyp4a14*) were markedly increased in the presence of shSrebp-1c (Supplementary Fig. 3). This indicates that the ChREBPα-driven FAO activation that we observe is not a general response to suppressed DNL in hepatocytes.

Lastly, we examined the physiological role of ChREBPα-driven FAO pathway in fasted or refed mice. 12-hr fasting significantly induced the mRNA levels of hepatic FAO genes such as *Cpt1a, Acadm, and Ehhadh* in *Chrebpα*-WT mice but not in *Chrebpα-LKO* mice (Supplementary Fig. 4), suggesting that hepatocyte ChREBPα partially contributes to fasting-induced FAO in the mouse liver.

### 2.2. ChREBPα promotes hepatocyte FAO independently of its DNA-binding ability

The canonical action of ChREBPα is as a transcription activator of *de novo* lipogenesis in response to fructose or glucose intracellular influx [33,42]. It seemed paradoxical for ChREBPα to function as a direct transcriptional activator of FAO genes. Moreover, we examined a previously published ChIP-seq dataset [43] of ChREBPα and could not find evidence supporting direct genomic binding of ChREBPα on the promoters of classical FAO genes (*Cpt1a, Ehhadh,* and *Acox1*). Therefore we hypothesized that ChREBPα may promote hepatocyte FAO independently of its DNA-binding ability. To test this hypothesis, we generated a mutant of ChREBPα that is incapable of inducing lipogenic gene expression due to an alanine (A)-glycine (G) mutation in its DNA binding motif(ChREBPα-

 © 2024 The Authors. Published by Elsevier GmbH. This is an open access article under the CC BY-NC-ND license (http://creativecommons.org/licenses/by-nc-nd/4.0/).

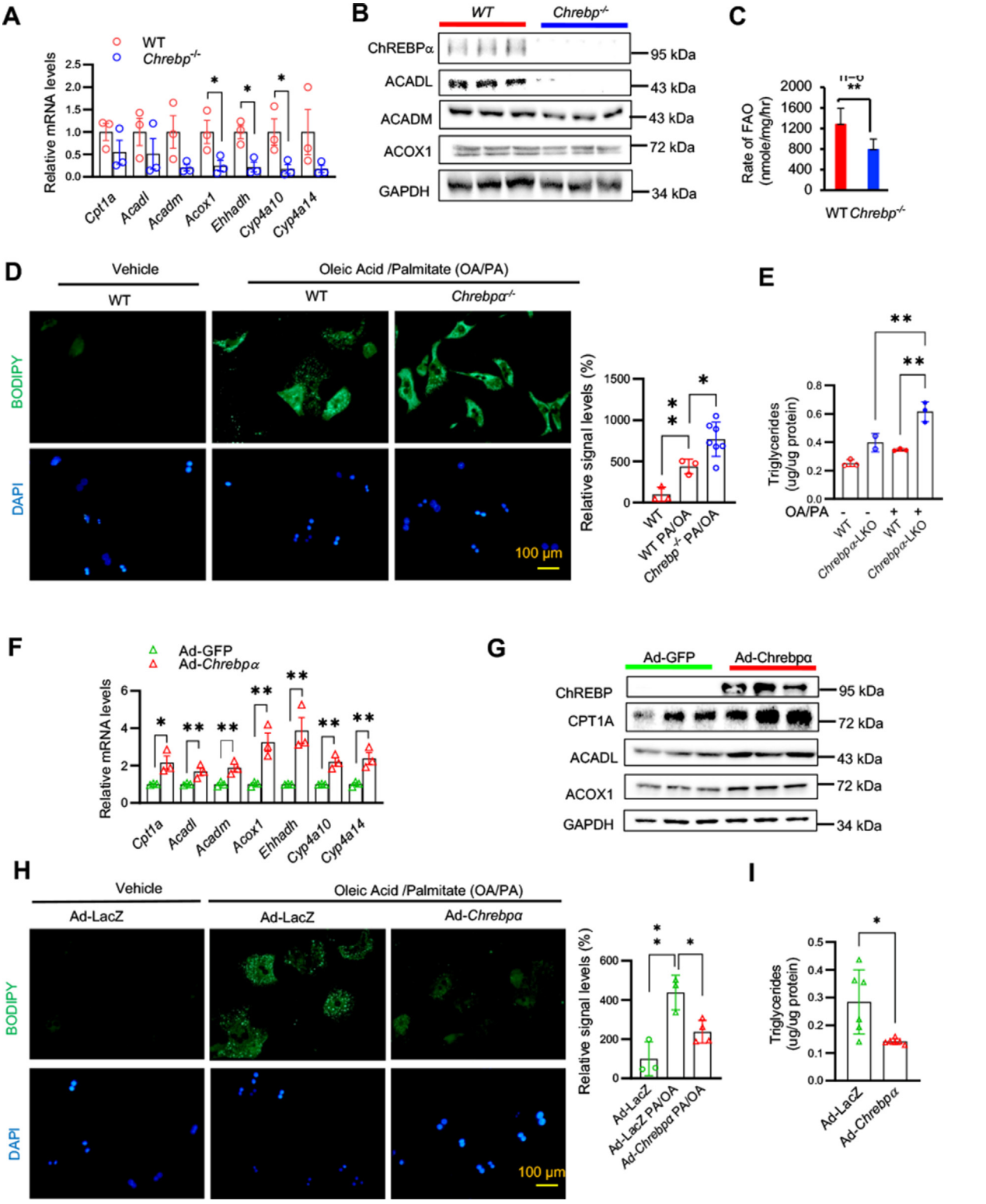


**Figure 1: ChREBPα is both necessary and sufficient to promote fatty acid oxidation in mouse hepatocytes.** Primary mouse hepatocytes (PMHs) were isolated from 8wk-old *Chrebp*$^{-/-}$ and WT littermates and cultured in serum-free medium for 24 h later prior to RT-qPCR for and immunoblotting to assess the expression of genes of FAO **(A**–**B)** as well as incubation with $H^3$-palmitate for 4 h before the measurement of the rate of FAO (**C**). WT and *Chrebp*$^{-/-}$ PMH were cultured in MEM medium with 300 μM palmitate and 600 μM oleate for 8 h, then switched to serum-free MEM medium for 16 h before lipid droplet detection by BODIPY staining (**D**) and cellular triglycerides assay (**E**). WT PMHs were isolated and transduced with either Ad-GFP control *vs.* Ad-*Chrebpα*. FAO enzyme expression was assessed by RT-qPCR and immunoblotting (**F-G**), while lipid content was measured by BODIPY staining and cellular TG assay after palmitate/oleate incubation (**H**–**I**). The data were plotted as Mean ± SEM (n = 3). $*p < 0.05$, $**p < 0.01$ by the Student's *t*-test.

 © 2024 The Authors. Published by Elsevier GmbH. This is an open access article under the CC BY-NC-ND license (http://creativecommons.org/licenses/by-nc-nd/4.0/).

AG), originally generated and described by the Towle group [44]. Compared with *Chrebpα-WT*, overexpression of ChREBPα-AG failed to activate luciferase reporters driven by the promoters of target genes *Lpk* or *Fasn*, which is consistent with deficient DNA binding and resulting reduced expression of other lipogenic targets (Supplementary Figs. 5A—B). In contrast, when either ChREBPα-WT or AG mutant were overexpressed in Huh7 hepatocytes, we observed increased CPT1A and ACADM protein expression, and reduced lipid droplet formation (Supplementary Fig. 6A-B). Taken together, we presented evidence showing ChREBPa promotes the hepatocyte FAO pathway independently of its DNA-binding ability and lipogenic activity.

### 2.3. Suppression of hepatic ChREBPα in liver with inflammation and fibrosis

We and others found that the intake of high-carbohydrate food or fructose-rich drinks induced hepatic ChREBPα expression [45—47]. However, the regulation of hepatic ChREBPα in the context of liver inflammation and fibrosis has not been reported. We firstly found that the combination of a lipotoxicity inducer (300 μM of palmitate) and an inflammatory cytokine (10 ng/ml of TNFα) markedly reduced the levels of ChREBPα but not SREBP-1c, another major lipogenic transcription factor (Figure 2A). The induction of p38 phosphorylation confirmed the positive stress response to palmitate/TNFα (Figure 2A). Next, we examined liver ChREBPα in mouse models of MASLD/MASH. Nuclear ChREBPα but not SREBP-1c was greatly reduced (up to 70%) in the liver of mice following a 10 week high fructose, methionine and choline-deficient (HFLMCD) diet (Figure 2B). Of note, HFLMCD diet is commonly used to induce full-blown MASH within 10 weeks of feeding in WT mice without causing body weight loss [48,49]. Moreover, we found that mice fed with just 7 days of HFLMCD exhibited liver injury and liver steatosis, markers of liver inflammation and fibrosis (Supplementary Figs. 7A—D). In the same liver, nuclear ChREBPα was reduced whereas nuclear SREBP1c was elevated (Supplementary Fig. 7E), suggesting that hepatic ChREBPα abundance is inversely associated with liver inflammation and fibrosis.

Next, we fed WT mice a MASH diet that is high in cholesterol, saturated fat, and fructose for 0, 3, 6, 12,15, and 20 weeks and examined the dynamics of liver ChREBPα and SREBP-1c protein levels. We chose this MASH diet because it largely mimics the diet of human NASH patients [50,51]. Of note, it takes at least 15 weeks of feeding for mice to develop inflammation and fibrosis [52,53]. During this time course, the nuclear abundance of ChREBPα was transiently increased between 6 and 12 weeks but dampened after 15 weeks. In contrast, nuclear SREBP-1c was up as early as 3 weeks and stayed elevated throughout the rest of the feeding period except for week 15 (Figure 2C). Lastly, we examined mRNA expression of *ChREBP* in normal control, steatotic, and MASH human livers. Consistent with the literature, several markers for liver fibrosis including *COL1A1, α-SMA,* and *TIMP1* were significantly upregulated in steatosis and further increased in MASH samples *vs.* normal liver tissues [54,55]. Liver *ChREBP* mRNA decreased in both steatotic and MASH liver samples, and was inversely associated with expression of the fibrosis markers. In contrast, liver *SREBP1* mRNA was significantly elevated in human MASH (Figure 2D). In summary, liver ChREBPα protein is markedly reduced in the liver of mouse models with MASH, consistent with reduced *Chrebpα* in human NASH liver. In the same setting, nuclear SREBP-1c is elevated in mouse and human MASH livers.

### 2.4. Hepatocyte *Chrebpα* deficiency leads to early onset of diet-induced MASH

Even though acute knockdown of liver *Chrebpα* using adenoviral transduction in *db/db* mice results in improved insulin sensitivity, glucose metabolism, and liver steatosis [37], the pathogenic role of hepatocyte ChREBPα in diet-induced MAFLD/MASH remains unclear. To examine how hepatocyte *Chrebpα* deficiency in adult mice impacts the onset and progression of this disease, we took advantage of AAV to generate adult-onset hepatocyte-specific *Chrebpα* knockout (*Chrebpα-LKO*) mice [56]. This approach allowed us to bypass any developmental defects due to the loss of hepatocyte ChREBPα. The loss of nuclear *Chrebpα* was confirmed by immunoblotting in liver tissues from $Chrebp\alpha^{flox/flox}$ mice injected with AAV-TBG-Cre (Figure 3A). Following 20 weeks of MASH diet feeding, both *Chrebpα-LKO* and control groups gradually gained weight at a similar rate (Figure 3B). However, *Chrebpα-LKO* mice showed more severe liver injury, as assessed with serum ALT and LDH at 12 weeks and 20 weeks of MASH diet feeding compared with control mice (Figure 3C—D). The total liver TG content showed an upward trend in the liver of *Chrebpα-LKO* mice without reaching statistical significance (Figure 3E). Total liver cholesterol was significantly higher in *Chrebpα-LKO* mice at the 12 week timepoint only (Figure 3F). Liver sections showed increased lipid droplets by H&E staining, inflammation by F4/80 immunohistochemistry staining, liver fibrosis by Sirius Red staining analyzed with Brunt Scoring system [57], and apoptosis by TUNEL staining (Figure 3G). Moreover, the RNA-seq analysis highlighted the enrichment of proinflammatory pathways (*Cxcl10, Ccl2, Ccl5, Nlrp3 and Tlr9*) as well as classical genes that indicate hepatic stellate cell activation and fibrosis (*Col1a1, Col3a1, Tgfβ1, Shh, Mmp12, and Plau*) in *Chrebpα-LKO* mouse livers compared with controls (Figure 3H). Some of these markers were also elevated in the liver of *Chrebpα-LKO* mice after 12 weeks of MASH diet (Supplementary Fig. 8). Lastly, the total protein levels of α-SMA and Vimentin, the two classical markers for hepatic stellate cell activation during liver fibrosis, were significantly elevated in the livers of *Chrebpα-LKO* mice after 20-wk NASH diet (Figure 4I). Taken together, our findings demonstrate that the loss of hepatocyte *Chrebpα* sensitizes mice to MASH diet-induced liver steatosis, hepatocyte injury, liver inflammation, and fibrosis.

### 2.5. Hepatic overexpression of ChREBPα protects mice against HFLMCD diet-induced MASH

Given the potent reduction of ChREBPα protein in MASH liver and its role in promoting hepatic FAO, we hypothesized that restoring liver ChREBPα expression might mitigate liver steatosis, hepatocyte injury, and fibrosis in WT mice with pre-existing MASLD/MASH induced by HFLMCD. To this end, WT male mice were fed the HFLMCD for 3 weeks prior to tail vein injection of Ad-GFP, Ad-Chrebpα-WT, or Ad-Chrebpα-AG. All groups of mice were on HFLMCD diet for 2 more weeks before sacrifice. The levels of liver ChREBPα were examined by immunoblotting to confirm the restoration of ChREBPα protein (Figure 4A). When compared with the Ad-GFP group, Ad-Chrebpa-WT and Ad-Chrebpα-AG mice showed reduced levels of total TG but not cholesterol in the liver (Figure 4B—C). This reduction in liver steatosis was accompanied with reduced hepatocyte injury measured by serum ALT (Figure 4D). H&E staining showed reduced lipid content and improved liver histology. TUNEL staining showed barely detectable hepatocyte apoptosis when ChREBPα-WT or -AG mutant was over-expressed, indicating that this protective role of ChREBPα is independent of its lipogenic action (Figure 4E). Restoration of ChREBPα expression also reduced liver fibrosis and inflammation, as shown by Sirius-Red staining and F4/80 immunohistochemistry staining, respectively (Figure 4E). Lastly, the total protein levels of α-SMA were significantly reduced in both ChREBPα WT and AG-injected mouse liver (Figure 4F). In summary, our data show that restoring hepatocyte ChREBPα expression in mice with pre-existing MASH not only markedly

 © 2024 The Authors. Published by Elsevier GmbH. This is an open access article under the CC BY-NC-ND license (http://creativecommons.org/licenses/by-nc-nd/4.0/).

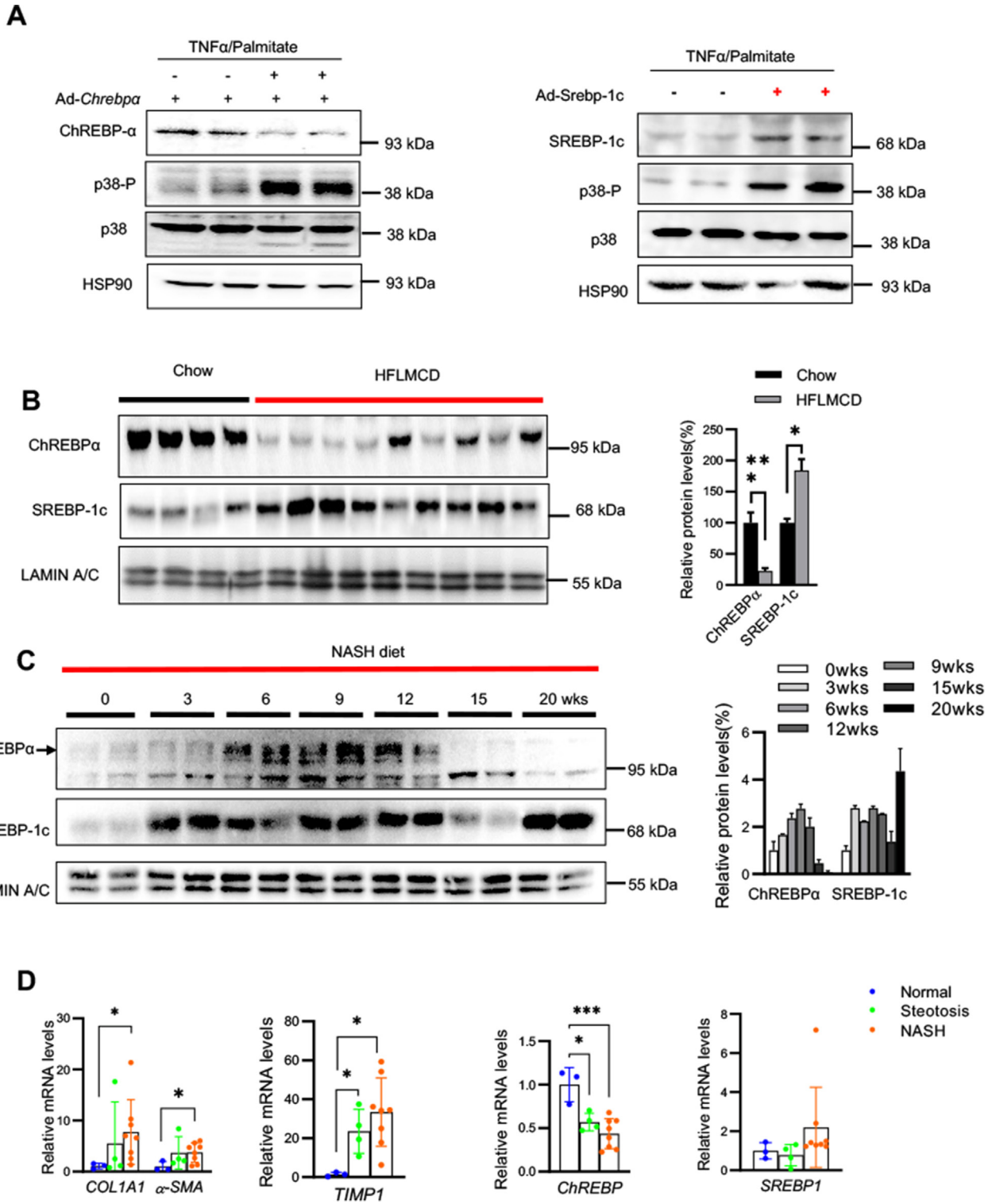


**Figure 2: Hepatic ChREBP$\alpha$ is suppressed in the liver of mouse models with diet-induced NASH and human patients of NASH**. WT PMHs from male mice were firstly transduced with either Ad-Chrebpα (**A**) or Ad-Srepb-1c (**B**) prior to treatment with TNF-α (10 ng/ml) plus palmitate (300 μM). The protein levels of ChREBPα or SREBP-1c were determined by immunoblotting. (**C**) Nuclear fractions of the liver samples of mice fed either regular chow *vs.* HFLMCD diet for 10 weeks or (**D**) mice fed NASH diet for 0, 3, 6, 9, 12, 15, or 20 weeks. The nuclear abundance of ChREBPα and SREBP-1c were determined by immunoblotting. (**E-F**) Livers samples form patients at different stages of NAFLD (Normal, Steatosis, and NASH) were subjected to RT-qPCR to exam the expression levels of fibrosis markers (*COL1A1*, *α-SMA, and TIMP1*) and *ChREBP* and *SREBP-1*. The data were plotted as mean ± SEM. $^{*}p < 0.05$, $^{****}p < 0.0001$ by the Student's *t*-test for **B**, and by one-way ANOVA for **D**.

 © 2024 The Authors. Published by Elsevier GmbH. This is an open access article under the CC BY-NC-ND license (http://creativecommons.org/licenses/by-nc-nd/4.0/).

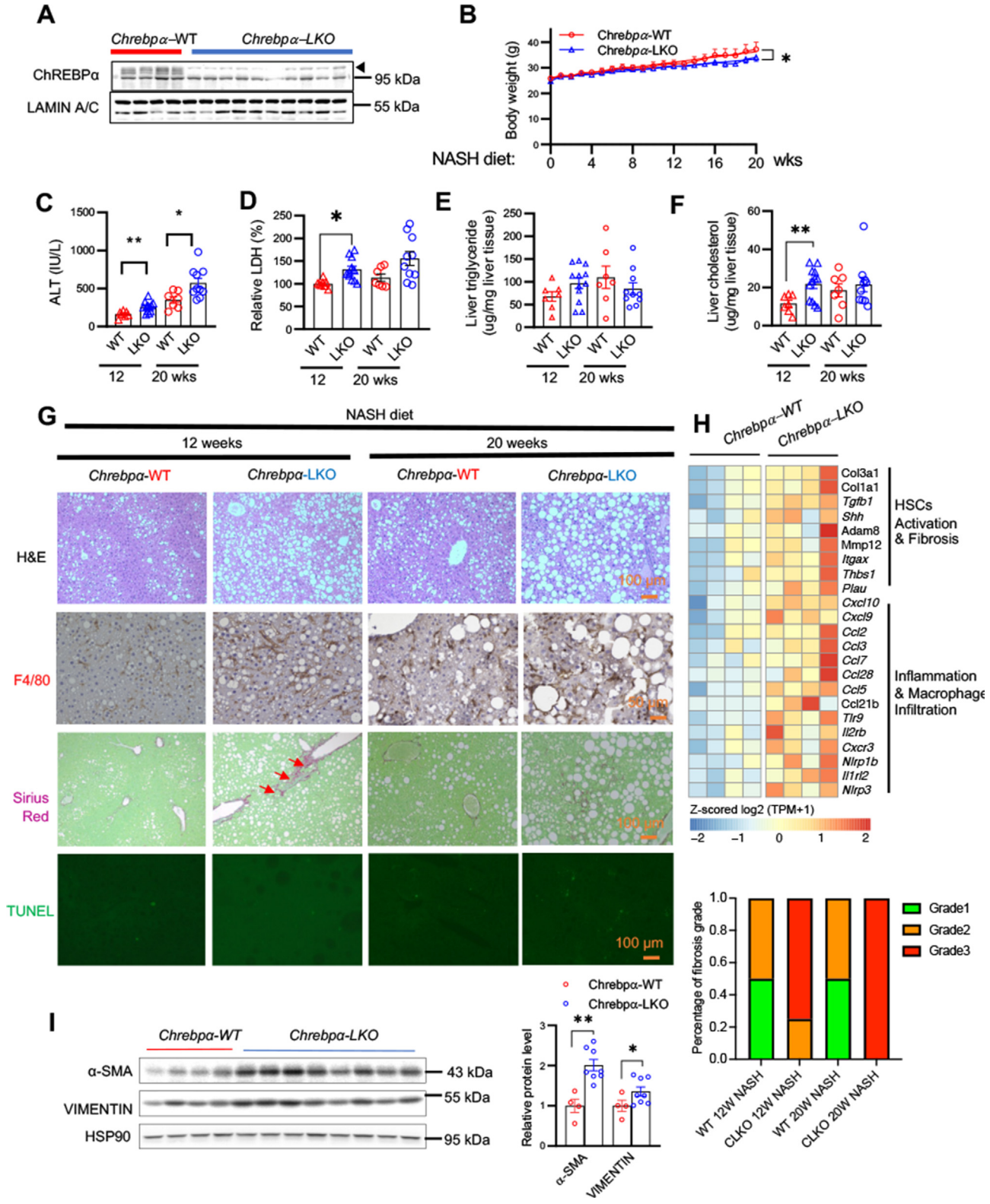


**Figure 3: Adult-onset deletion of hepatic *Chrebpα* sensitizes mice to NASH diet-induced liver steatosis**. 8-wk old *Chrebpα*$^{flox/flox}$ mice on regular chow were injected with AAV-TBG-*Cre* (*Chrebpα-LKO*) or AAV-TBG-GFP (*Chrebpα*-WT) via tail vein, and 2 weeks later, the mice were switched to NASH diet. (**A**) Western blot against ChREBPα was used to confirm *Chrebpα* deletion. (**B**) Body weight was monitored weekly. **(C–D)** Serum ALT and LDH at 12 weeks and 20 weeks of NASH diet feeding, (**E-F**) liver triglyceride and cholesterol. (**G**) H&E staining, F4/80 immunohistochemistary, Sirius Red staining, and TUNEL staining were used to detect lipid droplets, macrophage, fibrosis and apoptosis, respectively. (**H**) RNAs-seq analysis of liver tissue from *Chrebpα*-LKO and *Chrebpα*-WT mice fed NASH diet for 20 weeks. Heat-map of DGE associated with liver fibrosis and inflammation/macrophage infiltration was generated. (**I**) Western blot against α-SMA and Vimentin was used to assess fibrosis. The data were plotted as Mean ± SEM. $^{*}p < 0.05$, $^{**}p < 0.01$, & $^{****}p < 0.0001$ by linear regression for **B**, by one-way ANOVA for **C**, **D** &**F**, and by the Student's *t*-test for **I.**

 © 2024 The Authors. Published by Elsevier GmbH. This is an open access article under the CC BY-NC-ND license (http://creativecommons.org/licenses/by-nc-nd/4.0/).

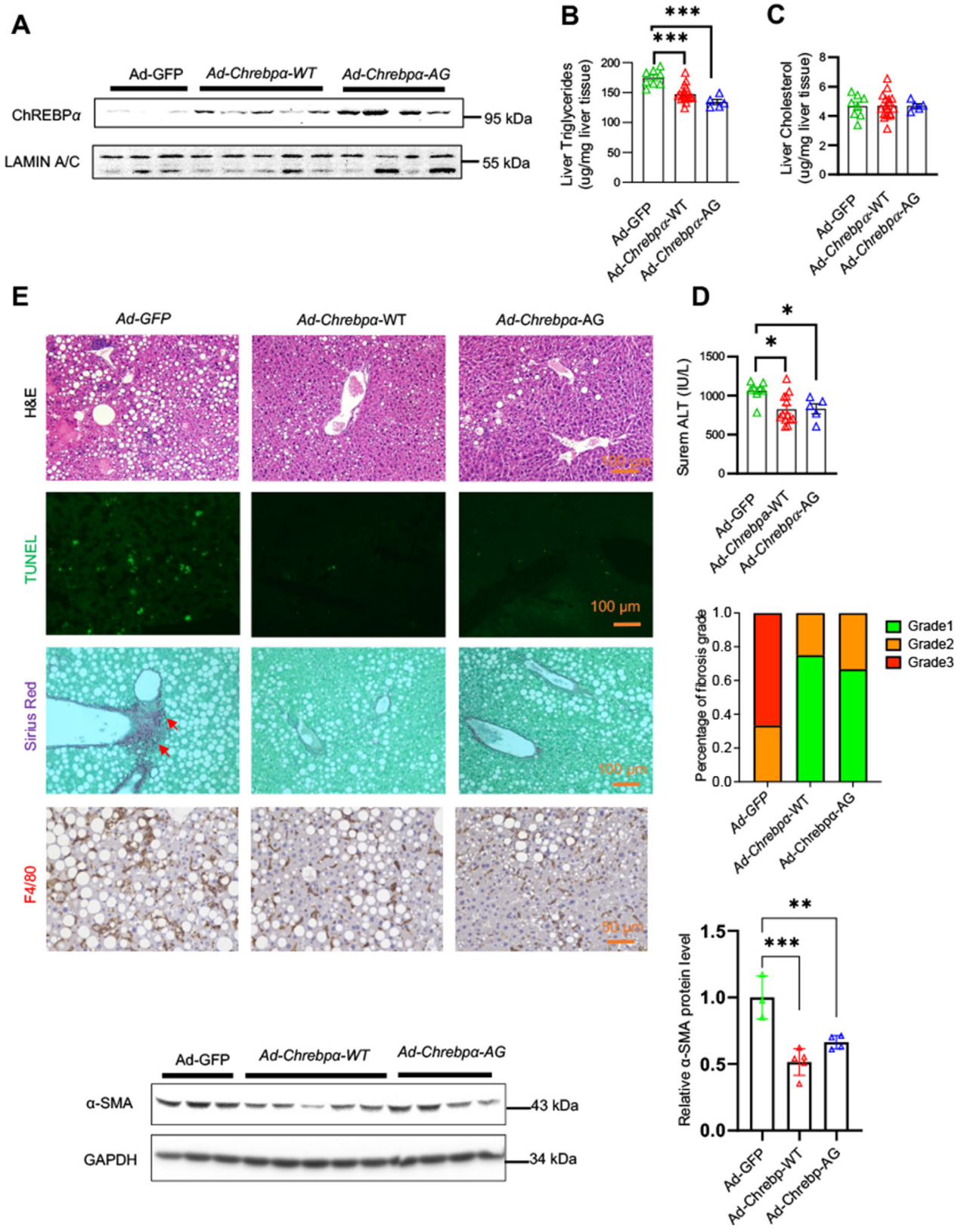


**Figure 4: Hepatic ChREBPα overexpression ameliorates liver steatosis and hepatocyte injury in mice with pre-existing NASH independently of its lipogenic action**. 8-wk old wildtype male mice fed HFLMCD diet for 2 weeks, and then injected with or Ad-GFP (n = 8), Ad-*Chrebpα*-WT (n = 17), or Ad-*Chrebpα*-AG (n = 5) via tail vein. After another week of HFLMCD feeding, (**A**) Confirmation of hepatic ChREBPα overexpression by immunoblotting, (**B**–**C**) liver triglycerides and cholesterol, (**D**) serum ALT. (**E**) H&E staining, F4/80 immunohistochemistry, Sirius Red staining and TUNEL staining were used to detect lipid droplets, macrophage infiltration, fibrosis, and apoptosis, respectively. (**F**) Protein levels of α-SMA in the liver by immunoblotting. The data were plotted as Mean ± SEM. $^{*}p < 0.05$, $^{**}p < 0.01$ & $^{***}p < 0.001$ by one-way ANOVA.

 © 2024 The Authors. Published by Elsevier GmbH. This is an open access article under the CC BY-NC-ND license (http://creativecommons.org/licenses/by-nc-nd/4.0/).

abrogates liver steatosis and hepatocyte injury but also improves liver fibrosis and inflammation, which supports the therapeutic potential of hepatocyte ChREBPα against MASH.

### 2.6. Role of hepatic ChREBPa in regulating the liver FAO pathway during diet-induced MASH

The canonical action of ChREBPα is to sense the intracellular influx of simple sugars and promote lipogenesis [33]. Unexpectedly, hepatocyte *Chrebpa* deficiency did not reduce mRNA and protein of DNL enzymes following 12 weeks of the MASH diet (Supplementary Figs. 9A—B). Moreover, hepatocyte *Chrebpa* deficiency did not impact mRNA levels of lipolysis (*Atgl* and *Lipe*), lipid uptake (*Cd36*), and lipid droplet binding proteins (*Fsp27b* and *Plin2*) (Supplementary Figs. 9C—E).

We have shown that, at least in cultured hepatocytes, ChREBPα is both necessary and sufficient to drive FAO, a catabolic pathway of fatty acid metabolism (Figure 1A—C). We also showed that hepatic *Chrebpα* deficiency partially impairs the fasting-induced FAO pathway in the liver of WT mice (Supplementary Fig. 4C). We were intrigued whether ChREBPα is also important for FAO gene expression in the context of diet-induced MASH. When compared with WT mice fed with MASH diet for 12 weeks, the expression of *Cpt1* and *Ehhadh* were significantly reduced in the liver of *Chrebpα-LKO* mice (Figure 5A—B). Similar findings were observed in the liver of mice fed 20 weeks of MASH diet with the expression of CPT1A being potently reduced in the liver of *Chrebpα-LKO* mice (Figure 5C—D). Conversely, overexpression of either ChREBPα-WT or AG mutant elevated the hepatic mRNA and protein levels of *Cpt1a*, *Ehhadh,* and *Acadm* in HFLMCD diet-fed mice (Figure 5E—F) with little effects on lipogenic and lipolysis pathways (Supplementary Fig. 10). In summary, our data showed that hepatocyte *Chrebpα* deficiency impairs the FAO pathway in both the fasting state and during MASH diet feeding, whereas its overexpression promotes the liver FAO pathway in mice with pre-existing MASH, suggesting that ChREBPα is both necessary and sufficient to activate the FAO pathway in the context of chronic liver injury.

It is well established that PPARα drives the hepatocyte FAO pathway during fasting [6]. Interestingly, the Postic group showed that ChREBPα cooperates with PPARα on glucose-induction of FGF21 expression, suggesting crosstalk between the two transcription factors to regulate FAO [58]. Indeed, we found that overexpression of ChREBPα significantly reduced the amount of lipid droplets in PMHs transduced with Ad-shLacZ. However, such effects were nearly abolished in cells transduced with Ad-shPparα, supporting that PPARα plays a major role in ChREBPα-driven FAO at least *in vitro* (Figure 5G).

### 2.7. ChREBPα is a novel regulator of the CYP450 epoxygenase pathway of arachidonic acid metabolism in the liver

How exactly ChREBPα impacts PPARα activity remains unexplored. Our unpublished data showed no major differences between WT and *Chrebpα-LKO* mice in terms of hepatic *Pparα* expression, raising the possibility that ChREBPα could regulate the PPARα activity through its ligands. To test this hypothesis, we firstly examined whether synthetic PPARα agonists could restore the FAO gene in *Chrebp*$^{-/-}$ PMHs. We used GFT505 (also called Elafibranor), a dual agonist of PPARα and δ since GFT505 has been shown to improve MASH in mice and human patients in a clinical trial [25]. Compared with the vehicle-treated *Chrebp*$^{-/-}$ PMHs with markedly reduced mRNA expression of FAO enzymes, GFT505-treated *Chrebp*$^{-/-}$ PMHs demonstrated completely restored levels of those genes (Supplementary Figs. 11A—B). Furthermore, either PPARa-specific agonist WY14643 [59] or PPARd-specific agonist GW501516 [60] could restore the protein expression of CPT1a, EHHADH, and ACADM in Huh7 cells with *Chrebpα* depletion (Supplementary Fig. 11C). In contrast, inhibition of PPARd by its specific antagonist GSK0660 [61] modestly impairs the ChREBPα ability's to promote FAO (Supplementary Fig. 11D). These findings have established a functional link between ChREBPα and the PPARα-driven FAO pathway, possibly via ChREPBα-mediated production of endogenous ligands for PPARa.

To gain molecular insights into the cell-autonomous action of ChREBPα in promoting hepatocyte FAO pathway, we performed pathway analysis of the RNA-seq data from livers of *Chrebpα-WT vs. Chrebpα-LKO* mice following 20-wk MASH diet as well as livers of Ad-GFP *vs.* Ad-Chrebpα after 2-wk HFLMCD diet. Several pathways were identified following the manipulation of ChREBPα and diet (Figure 6A—B). It is no surprise that fatty acid metabolism is altered given that ChREBPα activity increases lipogenesis and FAO. Intriguingly, we identified the arachidonic acid metabolic pathway as one of the unique pathways significantly altered in both experimental groups. In particular, one of the key epoxygenases of arachidonic acid metabolism [62,63], *Cyp2c50*, was significantly reduced in *Chrebpα-LKO* mice but increased by about 7-fold in the liver of Ad-Chrebpα-injected mice (Figure 6 C-D). Moreover, in PMHs, we observed similar changes of *Cyp2c50* in response to overexpression or deletion of *Chrebpα* (Figure 6E—G), indicating that regulation of *Cyp2c50* by ChREBPa is a cell-autonomous event. Interestingly, *Cyp4f18*, one of the omega-hydroxylases [64], was suppressed by *Chrebpa* overexpression, suggesting that ChREBPa -mediated induction of *Cyp2c50* is highly specific. Of note, the expression of other *Cyp2C* enzymes including *Cyp2C55, Cyp2c29,* and *Cyp2c39* was elevated in the liver of *Chrebpa-LKO* liver after 12 weeks of MASH diet (Supplementary Fig. 12). Lastly, the mRNA expression of the human homolog of *Cyp2c50*, called *CYP2C19* [65], was markedly reduced in human steatosis and MASH liver samples (Figure 6H). Altogether, our data support that ChREBPα may stimulate hepatic FAO by activating *Cyp2c450* expression to regulate arachidonic acid metabolism.

### 2.8. *Cyp2c50* overexpression partially reverses liver steatosis, inflammation, and fibrosis in mice with pre-existing NASH

We firstly asked if restoring *Cyp2c50* expression in *Chrebpα*-deficient PMHs is sufficient to restore the FAO pathway. To this end, we transduced *Chrebpα-LKO* PMH with Ad-Cyp2c50 that induced *Cyp2c50* by about 10-fold compared with Ad-LacZ control (Figure 7A). In this condition, the mRNA of several FAO enzymes, especially *Acadm* and *Acox1*, were significantly elevated by Cyp2c50 overexpression (Figure 7B). BODIPY staining showed that *Cyp2c50* overexpression reduced the accumulation of lipid droplets in *Chrebpα-LKO* PMH (Figure 7C). These *in vitro* findings suggest restoring *Cyp2c50* is sufficient to enhance the hepatocyte FAO pathway and reduce lipid droplet accumulation in the absence of ChREBPα. To test whether PPARα is required for CYP2C50-mediated FAO, we depleted *Pparα* in PMHs prior to overexpressing Cyp2c50. BODIPY staining showed that *Cyp2c50* overexpression reduced the accumulation of lipid droplets in WT PMH-transduced with Ad-shLacZ. However, such effects were largely abrogated in cells transduced with Ad-shPparα (Figure 7D).

Next we asked if hepatic Cyp2c50 is involved in diet-induced MAFLD in vivo. We first examined the expression of *Cyp2c50* in mouse models of diet-induced MAFLD/MASH. By RT-qPCR (the antibody against CYP2C50 is not available), we found that liver *Cyp2c50* mRNA levels were markedly downregulated in mice fed either 10 weeks of the HFLMCD (down to 10%) or 20 weeks of the MASH diet (down to 30%) (Supplementary Fig. 13). Thus we tested the therapeutic impact of

 © 2024 The Authors. Published by Elsevier GmbH. This is an open access article under the CC BY-NC-ND license (http://creativecommons.org/licenses/by-nc-nd/4.0/).

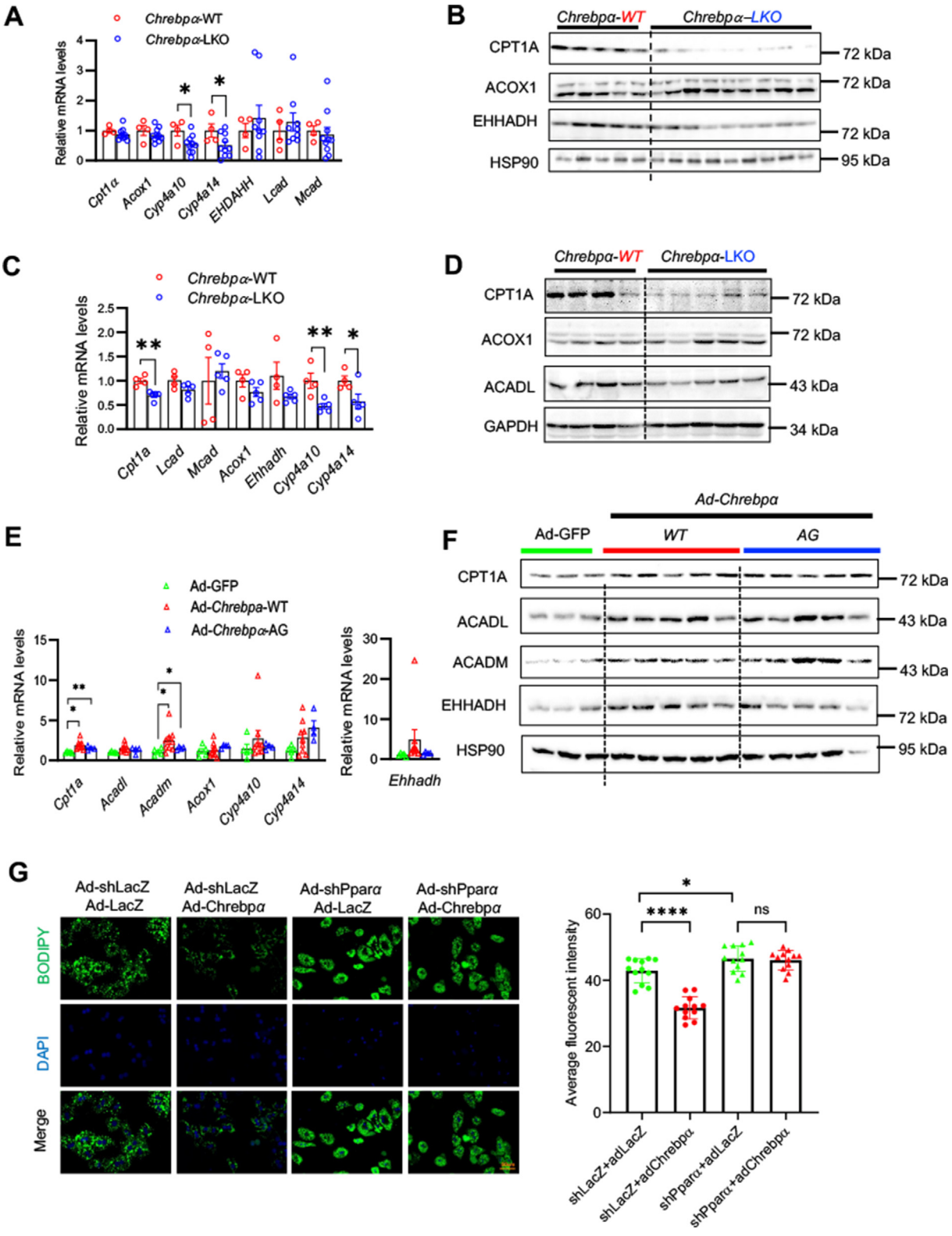


**Figure 5: Manipulations of hepatic ChREBPα impact FAO pathway in NASH.** (**A-D**) Hepatic *Chrebpα* deficiency impairs FAO in the liver. Liver tissues from *Chrebpα*-WT and *Chrebpα*-LKO mice fed NASH diet for 12 weeks (**A&B**) or 20 weeks (**C&D**) were subjected to RT-qPCR and western blot to assess the expression of FAO enzymes. (**E-F**) ChREBPα overexpression promotes FAO in the liver. Liver tissues from mice injected with Ad-GFP, Ad-*Chrebpα-WT,* or Ad-*Chrebpα-AG* and fed HFLMCD diet for 3 weeks were subjected to RT-qPCR and immunoblotting to assess FAO enzyme expression. (**G**) PMHs were transduced with either Ad-shLacZ or Ad-shPparα with or without Ad-*Chrebpα* prior to BODIPY staining. The data were plotted as Mean ± SEM. $^{*}p < 0.05$, $^{**}p < 0.01$ by the Student's *t*-test for **A&C,** by one-way ANOVA for **E**.

 © 2024 The Authors. Published by Elsevier GmbH. This is an open access article under the CC BY-NC-ND license (http://creativecommons.org/licenses/by-nc-nd/4.0/).

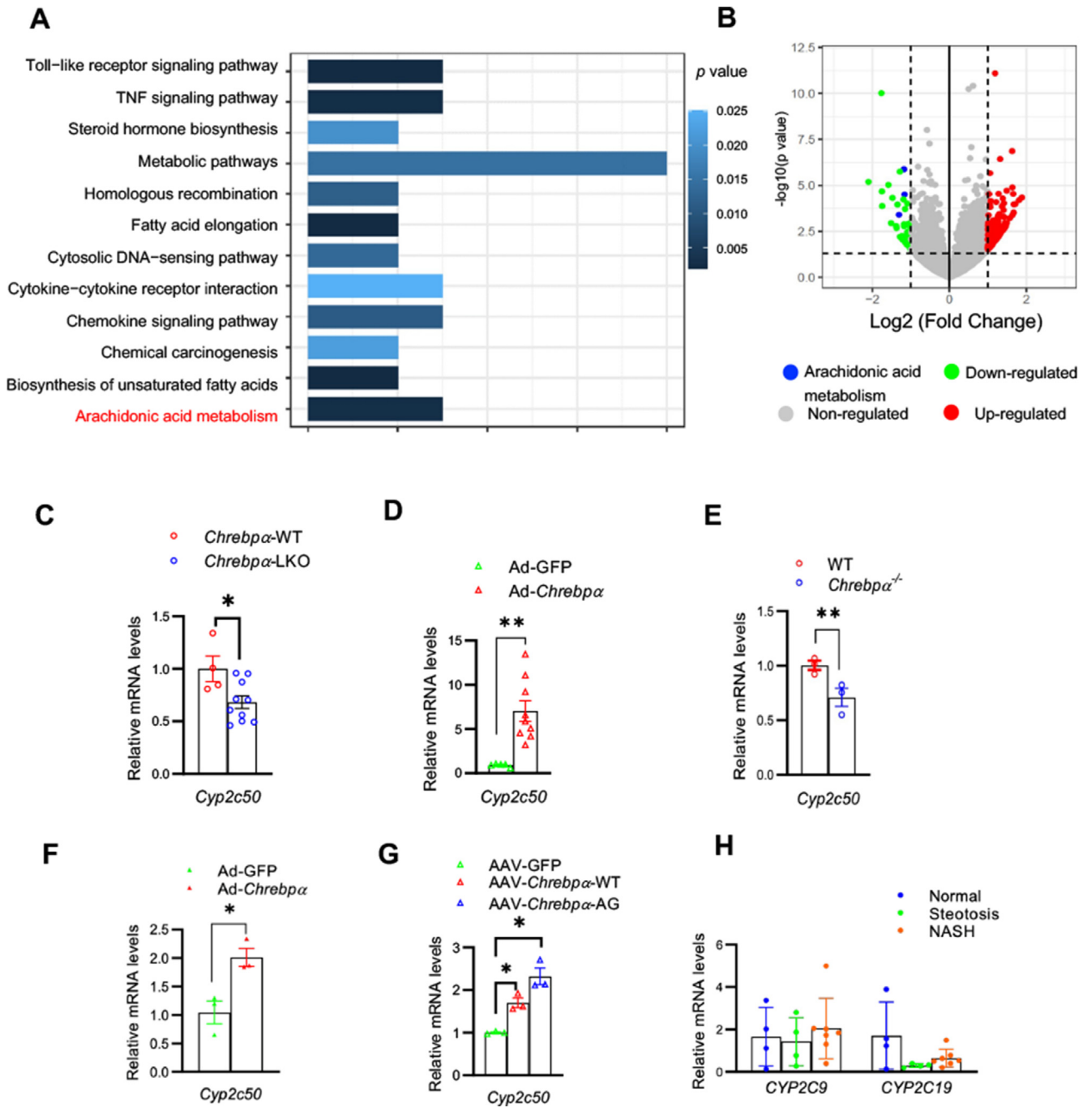


**Figure 6: Identification of epoxogenase pathway of arachidonic acid metabolism as a novel pathway of ChREBPα during diet-induced NASH**. Liver tissues from *Chrebpα*-LKO *vs. Chrebpα*-WT mice on NASH diet for 20 weeks, as well as liver tissues from WT mice fed 2-wk HFLMCD diet and injected Ad-Chrebpα *vs.* Ad-GFP were subjected to RNA-seq analysis (n = 4). (**A-B**) Regulation of epoxygenase pathway of the arachidonate metabolism by hepatic *Chrebpα* via Pathway Analysis. (**C**) Reduced hepatic *Cyp2c50* expression in *Chrebpα*-LKO mice following NASH diet; (**D**) Elevated hepatic *Cyp2c50* expression *in* Ad-GFP *vs.* Ad-Chrebpα-injected mice. (**E**) Decreased expression of hepatic *Cyp2c50* in *Chrebp*$^{-/-}$ mice. (**F**) *Cyp2c5*0 expression in Ad-GFP *vs.* Ad-Chrebpα PMHs, (**G**) *Cyp2c5*0 expression in PMHs from mice injected with AAV-TBG-GFP, AAV-TBG-*Chrebpα*-WT, or *Chrebpα*-AG. (**H**) Expression levels of *CYP2C9* and *CYP2C19* (the human ortholog of mouse *Cyp2c50)* in the liver of normal human *vs.* liver steatosis or NASH patients.

restoring *Cyp2c50* expression on liver steatosis, fibrosis, and inflammation in mice with pre-existing MASH. WT mice were fed the HFLMCD diet for 7 days before tail vein injection of Ad-Cyp2c50 *vs.* Ad-LacZ. 10 days later, Ad-Cyp2c50-injected mice showed about 2 fold increase in hepatic *Cyp2c50* expression (Figure 7E). In the same group of mice, *Cyp2c50* overexpression led to a significant reduction of serum ALT (Figure 7F) and liver TG (Figure 7G), but not liver cholesterol (Figure 7H). H&E staining showed reduced liver steatosis around the portal vein (Figure 7I). At the molecular level, we found the fibrosis markers, including *α-Sma* and *Col1a1,* mRNA levels were markedly reduced upon *Cyp2c50* overexpression (Figure 7J). Furthermore, we detected about 2 fold increase in the mitochondrial CPT1A protein level and significantly elevated total EHHADH and ACOX1 proteins (Figure 7K). Taken together, these in vivo findings highlighted the

 © 2024 The Authors. Published by Elsevier GmbH. This is an open access article under the CC BY-NC-ND license (http://creativecommons.org/licenses/by-nc-nd/4.0/).

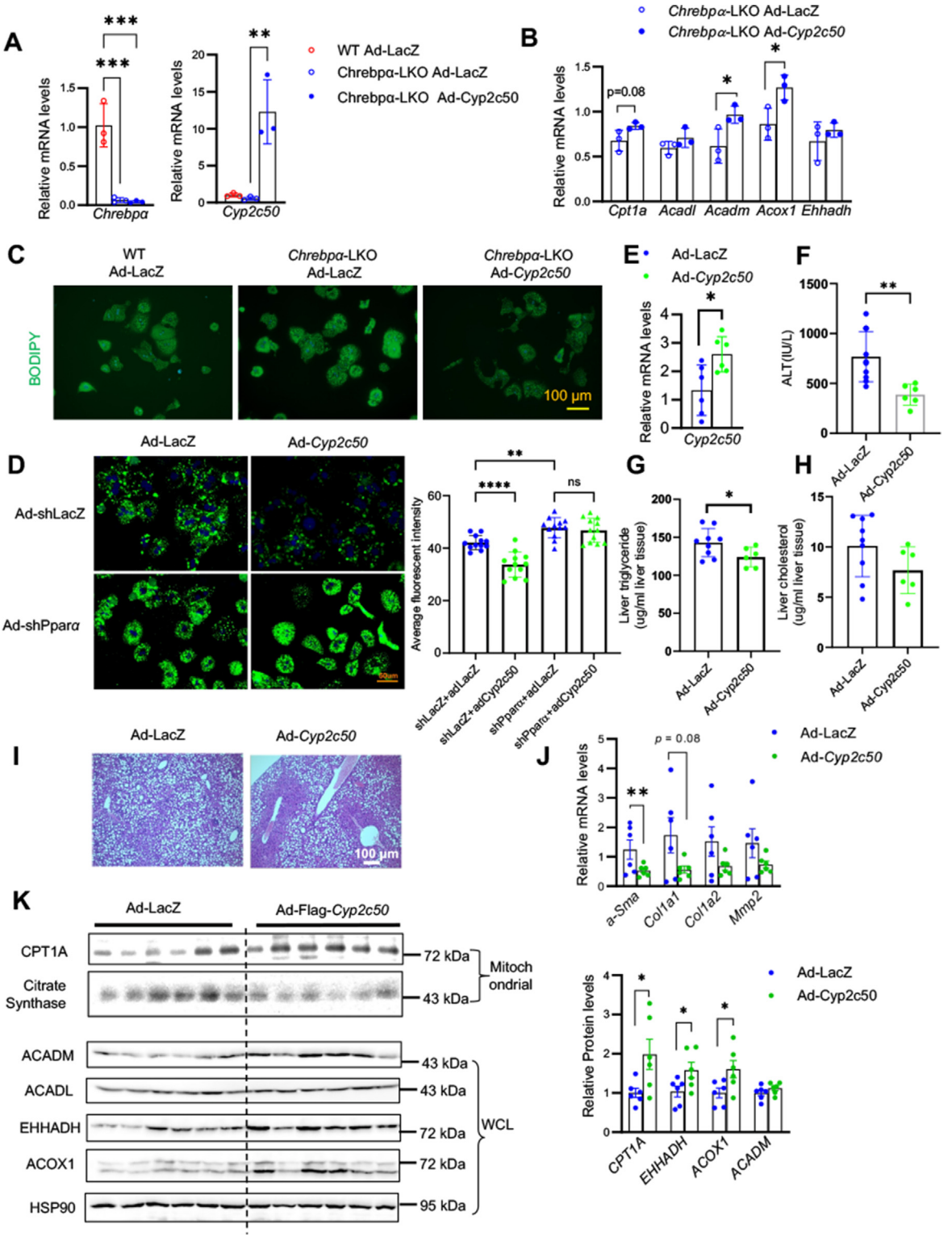


**Figure 7: Restoring CYP2c50 expression rescues FAO and alleviates diet-induced liver steatosis in *Chrebpα* deficient condition**. PMHs from *Chrebpα*-WT and *Chrebpα*-LKO mice were transduced with adenovirus overexpressing LacZ or *Cyp2c50*. The cells were harvested 24 h later for RT-qPCR to exam the expression levels of *Cyp2c50* and genes involved in FAO (**A-B**) and BODIPY (C) staining to assess lipid accumulation. (**D**) PMHs were transduced with either Ad-shLacZ or Ad-shPparα with or without *Ad-Cyp2c50* prior to BODIPY staining. *Chrebpα-LKO* mice were injected with Ad-*Cyp2c50* or Ad-LacZ. 2 days later, the mice were fed HFLMCD diet for 9 days, and then dissected. Liver *Cyp2c50* mRNA were measured by RT-qPCR (**E**). Liver injury was assessed by serum ALT (**F**), hepatic lipid content by liver triglycerides (**G**), cholesterol (**H**), and H&E staining (**I**), and the gene expression of hepatic fibrosis markers by RT-qPCR (**J**) and FAO enzymes by immunoblotting with quantification (**K**).

 © 2024 The Authors. Published by Elsevier GmbH. This is an open access article under the CC BY-NC-ND license (http://creativecommons.org/licenses/by-nc-nd/4.0/).

therapeutic potential of *Cyp2c50* activation in improving liver steatosis, reducing liver injury, and alleviating liver fibrosis possibly via restoring the hepatic FAO pathway.

## 3. DISCUSSION

Elevated *de novo* lipogenesis (DNL) is considered an important driver of MAFLD [5,9]. Hyperinsulinemia in metabolic syndrome leads to excessive hepatic DNL via activation of the LXRα-SREBP-1c cascade [66]. The Postic group showed that acute depletion of liver *Chrebp* in *ob/ob* mice markedly reduces liver DNL and lipid accumulation, supporting that ChREBP-driven DNL plays a crucial role in obese conditions due to loss of leptin signaling [37]. However, this might not be the case in mouse models of MASH. At least in mouse models of MASH that we examined, the nuclear abundance of ChREBPα is markedly reduced, whereas SREBP-1c is elevated, indicating that ChREBP is less relevant compared to SREBP-1c in the regulation of DNL in MAFLD. Meanwhile, our data with human MASH liver samples showed an inverse correlation between *ChREBPα* and the fibrosis marker *COL1A* in terms of the mRNA levels, consistent with previous findings [67]. Moreover, another study showed that hepatic ChREBP was increased in patients with liver steatosis but decreased in patients with severe insulin resistance [68], consistent with our time-course study of NASH diet feeding. Liver ChREBPα showed a bi-phasic pattern in which it was elevated during the first 12 weeks then dropped down to the basal level (Figure 2C). In contrast, liver SREBP-1c rose after 3 weeks of the MASH diet and remained elevated for the remainder of feeding. Such differential responses might explain steady or elevated levels of lipogenic genes in the liver of *Chrebpα-LKO* mice following 12-weeks and 20-weeks of the MASH diet (Supplementary Figs. 9A—B). So far, we have no evidence to suggest that elevated SREBP-1c is a consequence of ChREBPα inhibition in the liver undergoing metabolic and inflammatory stresses. We previously reported that ChREBPα promotes protein degradation of SREBP2 in response to fructose [46]. It is tempting to speculate that ChREBPα activity might have a similar effect on SREBP-1c in the context of metabolic and inflammatory stresses. Further detailed analysis of the dynamics between hepatocyte ChREBPα and SREBP-1c is warranted in the progression of NAFLD towards MASH.

In healthy conditions, the PPARα-dependent transcriptional activation of rate-limiting enzymes in FAO is necessary for hepatocytes to handle the influx of free fatty acids (FFA) during fasting [6,20,22]. However, in the presence of inflammatory and nutritional stresses, utilization of FFA by FAO is largely suppressed as a result of an impaired PPARα pathway [6,20]. Accumulated evidence suggest that PPARα's transcriptional activities are downregulated in mouse models of MASH due to [1] reduced expression of PPARα and its transcriptional coregulators and [2] elevated levels or activities of inhibitory regulators of PPARα [69—72]. In our current study, we revealed a novel mechanism for the suppression of PPARα-driven FAO by reducing the biosynthesis of its endogenous ligands [27,28]. We found that CYP2C50, one of the P450 epoxygenases of arachidonic acid metabolism, was potently reduced in the livers of mouse models of MASH, congruous with reduced hepatic FAO and the development of liver steatosis and fibrosis. In contrast, restoring hepatic CYP2C50 expression in mice with pre-existing NASH enhanced the FAO program and alleviated liver steatosis, fibrosis and injury. The P450 epoxygenase pathway leads to the formation the epoxyeicosatrienoic acids (EETs), which are further converted to dihydroxyeicosatrienoic acids (DHETs) by soluble epoxide hydrolase (sEH) [63,73]. EETs were found to potently activate PPARα at least in cell culture-based assays [28,74]. So far, it remains unclear about the identity of metabolites downstream of CYP2C50 that serve as endogenous ligands for hepatic PPARa. In addition to CYP2C50, it has been observed that the expression of other CYP epoxygenases, including *Cyp2c5*5 and *Cyp2c29,* was also potently reduced in mice fed an atherogenic diet [75]. The expression of these two enzymes was slightly increased in the liver of *Chrebpα-LKO* mice, indicating that the ChREBPα-driven *Cyp2c50* is highly specific and the inhibitory effect of downregulation of *Cyp2c50* on FAO could not be compensated by other CYP epoxygenases such as *Cyp2c55* or *Cyp2c29*, underscoring the physiologic importance of CYP2C50 as an endogenous activator of the PPARα-FAO pathway. Our current study supports that ChREBPα is both necessary and sufficient to promote hepatocyte *Cyp2c50* expression. Yet our ChREBPα AG-mutant data support that it does not require the ChREBPα's DNA-binding activity. Future research will examine non-canonical actions of ChREBPα on the expression of CYP2C50 and, subsequently, PPARα and FAO pathways.

Our RNA-seq analysis unveiled the impact of hepatocyte *Chrebpα* deficiency on the activation of hepatic stellate cells (HSCs) and elevated liver fibrosis. One possible explanation is the secondary response following reduced liver steatosis and liver injury. Another possibility is hepatocyte ChREBP might influence the liver microenvironment to regulate the activity of HSCs. This concept is supported by recent findings that hepatocyte-derived factors such as pro-fibrogenic cytokines, lipids, and ROS can directly activate HSCs [54,76]. For example, overactivation of hepatocyte NOTCH signaling promotes HSC activation by releasing excess osteoponitin [77]. Hepatocyte-derived IL-11 can directly activate quiescent HSCs via the ERK pathway [48]. We found via RNA analysis that the NASH diet elevates several hepatic profibrogenic factors (*Thbs1, Tgfb1, Ctgf* and *Shh*) [78—80] in *Chrebpα-LKO* mice, suggesting that hepatocyte ChREBPα may function as a non-cell autonomous regulator of HSC activation.

In this study, our extensive analysis performed in *Chrebp*$^{-/-}$ hepatocytes and *Chrebpα-LKO* mice has allowed us to identify the novel actions of ChREBPα in hepatocyte fatty acid metabolism. ChREBPα plays a surprisingly essential for FAO by potentially supporting CYP2C50-dependent biosynthesis of endogenous ligands for PPARα. Our work provides the first demonstration that hepatocyte-specific *Chrebpα* deletion impairs FAO and sensitizes mice to early onset of MASH, whereas hepatocyte-specific overexpression of ChREBPα enhances FAO and mitigates liver steatosis, hepatocyte injury, and fibrosis in mice with pre-existing MASH. These findings underscore the protective role of hepatocyte ChREBPα via its non-lipogenic actions against lipid overload and hepatocyte injury during MASLD. These data highlight the relevance of ChREBPα as a drug target for MAFLD treatment.

## 4. MATERIALS AND METHODS

### 4.1. Animal experiments

All animal experiments were approved by the Institutional Animal Care and Research Advisory Committee at the University of Michigan. *C57BL/6* mice were maintained on 12 h/12 h light/dark cycles with ad-lib access to food and water. *Chrebp*$^{flox/flox}$ mice were generously provided by Dr. Lawrence Chan, Dr. Pradip Saha, and Dr. Alli Antar at Baylor College of Medicine. Mice were fed MAFLD-inducing diets for specified durations and fasted for 6 h before dissection. MASH diet (D09100310, 40 kcal% Fat (Palm Oil), 20 kcal% Fructose and 2% Cholesterol) and HFLMCD (A06071309, 45 kcal% Fat, 0.1% Methionine and Choline deficient diet) were purchased from Research Diets. For liver specific overexpression, GFP, *Flag-Chrebpα*-WT, *Flag-Chrebpα*-AG, or *Cyp2c50* overexpressing adenoviruses were delivered via tail vein injection at the dose of $1 \times 10^{12}$ plaque-forming units. Liver tissues were harvested for histological analysis, mRNA, and

 © 2024 The Authors. Published by Elsevier GmbH. This is an open access article under the CC BY-NC-ND license (http://creativecommons.org/licenses/by-nc-nd/4.0/).

protein analysis. Frozen sections were used for TUNEL staining, while paraffin-embedded tissues were used for section and Haematoxylin and Eosin (H&E) staining, Picro-Sirius Red staining, and F4/80 staining. Detailed protocols for Picro-Sirius Red staining and F4/80 staining are available in the Supplemental Experimental Procedures.

### 4.2. RNA-seq analysis

Total RNA was extracted with RNeasy (QIAGEN, Cat. 74104) from livers of *Chrebp*$\alpha^{flox/flox}$ mice (n = 4) or *Chrebp*$\alpha$-LKO mice (n = 4) fed with MASH diet for 12 weeks, or livers of mice injected with Ad-GFP (n = 4) or Ad-*Chrebp*$\alpha$ (n = 4) fed with HFLMCD diet. RNA-seq libraries were prepared via the following workflow: mRNA enrichment, reverse transcription with N6 random primer, end repair, PCR amplification, denaturation and cyclization. Samples were processed on DNBseq platform to generate datasets of single-end 50bp reads. After reads filtering, clean reads were mapped to reference transcripts using Bowtie2. Then gene expression level for each sample was calculated with RSEM. Differentially expressed genes (DEG) were identified with DEseq2 algorithms. The heatmap was generated with heatmap R package to compare gene expression levels between NASH diet-fed *Chrebp*$\alpha^{flox/flox}$ mice *vs.* *Chrebp*$\alpha$-LKO mice, and between HFLMCD diet-fed Ad-GFP injected *vs.* Ad-*Chrebp*$\alpha$ injected mice. The KEGG pathway analysis was performed by using DAVID database and visualized by ggplot2 R package.

### 4.3. Data resource sharing and availability

All the data and critical resources supporting our findings as well as methods, and conclusions will be shared by the corresponding authors upon request. The original data of RNA-seq is available in the NCBI's Gene Expression Omnibus (GEO) database (GEO GSE223649).

### 4.4. Statistical analyses

Statistical analysis was performed using Prism version 6.0 (GraphPad Software, San Diego, CA). Statistical significance was determined either by unpaired two-tailed Student's *t*-test for comparison between two groups or by one-way *ANOVA* with Tukey's or Dunnett's post-hoc test for multiple group comparison. All results are given as the Mean $\pm$ SEM or Mean $\pm$ SD. Results were considered statistically significant with $p$ value $< 0.05$.
Additional methods are provided in Supplementary Materials.

## FUNDING

This work was supported by an R01 (DK099593) to L.Y. and an R01 (DK121170) to X.T. Part of the work was also supported by pilot grants from Michigan Nutrition Obesity Research Center (P30 DK089503 to L.Y. and X. T.), Michigan Diabetes Research Training Center (P60 DK020572 to L. Y., X.T., and D. Z.), Center for Gastrointestinal Research (P30 DK034993 to D.Z.). A. N.-A. was supported by a USDA-ARS Cooperative Agreement (3092-51000-064-005-S), an American Heart Association CDA (18CDA34110137), and a Texas Children's Hospital Pediatrics Pilot Award.

## CREDIT AUTHORSHIP CONTRIBUTION STATEMENT

**Deqiang Zhang:** Writing – original draft, Visualization, Investigation, Formal analysis, Data curation. **Yuee Zhao:** Visualization, Validation, Investigation, Formal analysis, Data curation. **Gary Zhang:** Resources, Methodology. **Daniel Lank:** Resources. **Sarah Cooke:** Resources. **Sujuan Wang:** Resources, Formal analysis. **Alli Nuotio-Antar:** Resources. **Xin Tong:** Writing – review & editing, Supervision, Resources, Funding acquisition, Formal analysis, Data curation, Conceptualization. **Lei Yin:** Writing – review & editing, Writing – original draft, Supervision, Resources, Project administration, Funding acquisition, Formal analysis, Conceptualization.

## ACKNOWLEDGMENTS

*Chrebpa*$^{flox/flox}$ mice were generously provided by Dr. Lawrence Chan from Baylor College of Medicine. The specimens used in this study were provided by the University of Kansas Liver Tissue Biorepository supported by grant IP20GM144269-01 from the NIH General Medical Science. The authors acknowledge the contribution of the patients who donated specimens for research as well as the physicians, nurses, and researchers who procured the specimens. The pcDNA-Cyp2c50 expression vector was generously provided by Dr. Darryl Zeldin from NIEHS at North Carolina.

## DECLARATION OF COMPETING INTEREST

We declare there is no conflict interest for this manuscript.

## DATA AVAILABILITY

Data will be made available on request.

## APPENDIX A. SUPPLEMENTARY DATA

Supplementary data to this article can be found online at https://doi.org/10.1016/j.molmet.2024.101957.

## REFERENCES

[1] Alves-Bezerra M, Cohen DE. Triglyceride metabolism in the liver. Compr Physiol 2017;8(1):1–8.
[2] Rui L. Energy metabolism in the liver. Compr Physiol 2014;4(1):177–97.
[3] Loomba R, Friedman SL, Shulman GI. Mechanisms and disease consequences of nonalcoholic fatty liver disease. Cell 2021;184(10):2537–64.
[4] Savage DB, Petersen KF, Shulman GI. Disordered lipid metabolism and the pathogenesis of insulin resistance. Physiol Rev 2007;87(2):507–20.
[5] Softic S, Cohen DE, Kahn CR. Role of dietary fructose and hepatic de novo lipogenesis in fatty liver disease. Dig Dis Sci 2016;61(5):1282–93.
[6] Bougarne N, Weyers B, Desmet SJ, Deckers J, Ray DW, Staels B, et al. Molecular actions of PPARalpha in lipid metabolism and inflammation. Endocr Rev 2018;39(5):760–802.
[7] Koonen DP, Jacobs RL, Febbraio M, Young ME, Soltys CL, Ong H, et al. Increased hepatic CD36 expression contributes to dyslipidemia associated with diet-induced obesity. Diabetes 2007;56(12):2863–71.
[8] Doege H, Grimm D, Falcon A, Tsang B, Storm TA, Xu H, et al. Silencing of hepatic fatty acid transporter protein 5 in vivo reverses diet-induced non-alcoholic fatty liver disease and improves hyperglycemia. J Biol Chem 2008;283(32):22186–92.
[9] Donnelly KL, Smith CI, Schwarzenberg SJ, Jessurun J, Boldt MD, Parks EJ. Sources of fatty acids stored in liver and secreted via lipoproteins in patients with nonalcoholic fatty liver disease. J Clin Invest 2005;115(5):1343–51.
[10] Begriche K, Massart J, Robin MA, Bonnet F, Fromenty B. Mitochondrial adaptations and dysfunctions in nonalcoholic fatty liver disease. Hepatology 2013;58(4):1497–507.
[11] Moore MP, Cunningham RP, Meers GM, Johnson SA, Wheeler AA, Ganga RR, et al. Compromised hepatic mitochondrial fatty acid oxidation and reduced markers of mitochondrial turnover in human NAFLD. Hepatology 2022;76(5):1452–65.

 © 2024 The Authors. Published by Elsevier GmbH. This is an open access article under the CC BY-NC-ND license (http://creativecommons.org/licenses/by-nc-nd/4.0/).

[12] Rector RS, Thyfault JP, Uptergrove GM, Morris EM, Naples SP, Borengasser SJ, et al. Mitochondrial dysfunction precedes insulin resistance and hepatic steatosis and contributes to the natural history of non-alcoholic fatty liver disease in an obese rodent model. J Hepatol 2010;52(5):727—36.
[13] Huang Y, Cohen JC, Hobbs HH. Expression and characterization of a PNPLA3 protein isoform (I148M) associated with nonalcoholic fatty liver disease. J Biol Chem 2011;286(43):37085—93.
[14] Kozlitina J, Smagris E, Stender S, Nordestgaard BG, Zhou HH, Tybjaerg-Hansen A, et al. Exome-wide association study identifies a TM6SF2 variant that confers susceptibility to nonalcoholic fatty liver disease. Nat Genet 2014;46(4):352—6.
[15] Longo M, Meroni M, Paolini E, Erconi V, Carli F, Fortunato F, et al. TM6SF2/PNPLA3/MBOAT7 loss-of-function genetic variants impact on NAFLD development and progression both in patients and in in vitro models. Cell Mol Gastroenterol Hepatol 2022;13(3):759—88.
[16] Schlaepfer IR, Joshi M. CPT1A-mediated fat oxidation, mechanisms, and therapeutic potential. Endocrinology 2020;161(2).
[17] Weber M, Mera P, Casas J, Salvador J, Rodriguez A, Alonso S, et al. Liver CPT1A gene therapy reduces diet-induced hepatic steatosis in mice and highlights potential lipid biomarkers for human NAFLD. FASEB J 2020;34(9):11816—37.
[18] Goedeke L, Bates J, Vatner DF, Perry RJ, Wang T, Ramirez R, et al. Acetyl-CoA carboxylase inhibition reverses NAFLD and hepatic insulin resistance but promotes hypertriglyceridemia in rodents. Hepatology 2018;68(6):2197—211.
[19] Tamura YO, Sugama J, Iwasaki S, Sasaki M, Yasuno H, Aoyama K, et al. Selective acetyl-CoA carboxylase 1 inhibitor improves hepatic steatosis and hepatic fibrosis in a preclinical nonalcoholic steatohepatitis model. J Pharmacol Exp Ther 2021;379(3):280—9.
[20] Pawlak M, Lefebvre P, Staels B. Molecular mechanism of PPARalpha action and its impact on lipid metabolism, inflammation and fibrosis in non-alcoholic fatty liver disease. J Hepatol 2015;62(3):720—33.
[21] Regnier M, Polizzi A, Smati S, Lukowicz C, Fougerat A, Lippi Y, et al. Hepatocyte-specific deletion of Pparalpha promotes NAFLD in the context of obesity. Sci Rep 2020;10(1):6489.
[22] Montagner A, Polizzi A, Fouche E, Ducheix S, Lippi Y, Lasserre F, et al. Liver PPARalpha is crucial for whole-body fatty acid homeostasis and is protective against NAFLD. Gut 2016;65(7):1202—14.
[23] Francque SM. Towards precision medicine in non-alcoholic fatty liver disease. Rev Endocr Metab Disord 2023;24(5):885—99.
[24] Francque SM, Bedossa P, Ratziu V, Anstee QM, Bugianesi E, Sanyal AJ, et al. A randomized, controlled trial of the pan-PPAR agonist lanifibranor in NASH. N Engl J Med 2021;385(17):1547—58.
[25] Ratziu V, Harrison SA, Francque S, Bedossa P, Lehert P, Serfaty L, et al. Elafibranor, an agonist of the peroxisome proliferator-activated receptor-alpha and -delta, induces resolution of nonalcoholic steatohepatitis without fibrosis worsening. Gastroenterology 2016;150(5):1147—1159 e1145.
[26] Wahli W, Michalik L. PPARs at the crossroads of lipid signaling and inflammation. Trends Endocrinol Metab 2012;23(7):351—63.
[27] Bishop-Bailey D, Wray J. Peroxisome proliferator-activated receptors: a critical review on endogenous pathways for ligand generation. Prostaglandins Other Lipid Mediat 2003;71(1-2):1—22.
[28] Wray JA, Sugden MC, Zeldin DC, Greenwood GK, Samsuddin S, Miller-Degraff L, et al. The epoxygenases CYP2J2 activates the nuclear receptor PPARalpha in vitro and in vivo. PLoS One 2009;4(10):e7421.
[29] Ng VY, Huang Y, Reddy LM, Falck JR, Lin ET, Kroetz DL. Cytochrome P450 eicosanoids are activators of peroxisome proliferator-activated receptor alpha. Drug Metab Dispos 2007;35(7):1126—34.
[30] Fang X, Dillon JS, Hu S, Harmon SD, Yao J, Anjaiah S, et al. 20-carboxy-arachidonic acid is a dual activator of peroxisome proliferator-activated receptors alpha and gamma. Prostaglandins Other Lipid Mediat 2007;82(1-4):175—84.
[31] Schuck RN, Zha W, Edin ML, Gruzdev A, Vendrov KC, Miller TM, et al. The cytochrome P450 epoxygenase pathway regulates the hepatic inflammatory response in fatty liver disease. PLoS One 2014;9(10):e110162.
[32] Arvind A, Osganian SA, Sjoquist JA, Corey KE, Simon TG. Epoxygenase-Derived epoxyeicosatrienoic acid mediators are associated with nonalcoholic fatty liver disease, nonalcoholic steatohepatitis, and fibrosis. Gastroenterology 2020;159(6):2232—2234 e2234.
[33] Iizuka K, Bruick RK, Liang G, Horton JD, Uyeda K. Deficiency of carbohydrate response element-binding protein (ChREBP) reduces lipogenesis as well as glycolysis. Proc Natl Acad Sci U S A 2004;101(19):7281—6.
[34] Filhoulaud G, Guilmeau S, Dentin R, Girard J, Postic C. Novel insights into ChREBP regulation and function. Trends Endocrinol Metab 2013;24(5):257—68.
[35] Ortega-Prieto P, Postic C. Carbohydrate sensing through the transcription factor ChREBP. Front Genet 2019;10:472.
[36] Wang H, Dolezal JM, Kulkarni S, Lu J, Mandel J, Jackson LE, et al. Myc and ChREBP transcription factors cooperatively regulate normal and neoplastic hepatocyte proliferation in mice. J Biol Chem 2018;293(38):14740—57.
[37] Dentin R, Benhamed F, Hainault I, Fauveau V, Foufelle F, Dyck JR, et al. Liver-specific inhibition of ChREBP improves hepatic steatosis and insulin resistance in ob/ob mice. Diabetes 2006;55(8):2159—70.
[38] Zarain-Herzberg A, Rupp H. Therapeutic potential of CPT I inhibitors: cardiac gene transcription as a target. Expert Opin Investig Drugs 2002;11(3):345—56.
[39] Moon YA. The SCAP/SREBP pathway: a mediator of hepatic steatosis. Endocrinol Metab (Seoul) 2017;32(1):6—10.
[40] Ferre P, Foufelle F. Hepatic steatosis: a role for de novo lipogenesis and the transcription factor SREBP-1c. Diabetes Obes Metab 2010;12(Suppl 2):83—92.
[41] Ferre P, Phan F, Foufelle F. SREBP-1c and lipogenesis in the liver: an update1. Biochem J 2021;478(20):3723—39.
[42] Yamashita H, Takenoshita M, Sakurai M, Bruick RK, Henzel WJ, Shillinglaw W, et al. A glucose-responsive transcription factor that regulates carbohydrate metabolism in the liver. Proc Natl Acad Sci U S A 2001;98(16):9116—21.
[43] Poungvarin N, Chang B, Imamura M, Chen J, Moolsuwan K, Sae-Lee C, et al. Genome-Wide analysis of ChREBP binding sites on male mouse liver and white adipose chromatin. Endocrinology 2015;156(6):1982—94.
[44] Ma L, Sham YY, Walters KJ, Towle HC. A critical role for the loop region of the basic helix-loop-helix/leucine zipper protein Mlx in DNA binding and glucose-regulated transcription. Nucleic Acids Res 2007;35(1):35—44.
[45] Softic S, Gupta MK, Wang GX, Fujisaka S, O'Neill BT, Rao TN, et al. Divergent effects of glucose and fructose on hepatic lipogenesis and insulin signaling. J Clin Invest 2017;127(11):4059—74.
[46] Zhang D, Tong X, VanDommelen K, Gupta N, Stamper K, Brady GF, et al. Lipogenic transcription factor ChREBP mediates fructose-induced metabolic adaptations to prevent hepatotoxicity. J Clin Invest 2017;127(7):2855—67.
[47] Fisher FM, Kim M, Doridot L, Cunniff JC, Parker TS, Levine DM, et al. A critical role for ChREBP-mediated FGF21 secretion in hepatic fructose metabolism. Mol Metabol 2017;6(1):14—21.
[48] Dong J, Viswanathan S, Adami E, Singh BK, Chothani SP, Ng B, et al. Hepatocyte-specific IL11 cis-signaling drives lipotoxicity and underlies the transition from NAFLD to NASH. Nat Commun 2021;12(1):66.
[49] Yang M, Zhang D, Zhao Z, Sit J, Saint-Sume M, Shabandri O, et al. Hepatic E4BP4 induction promotes lipid accumulation by suppressing AMPK signaling in response to chemical or diet-induced ER stress. FASEB J. 2020.
[50] Wang X, Zheng Z, Caviglia JM, Corey KE, Herfel TM, Cai B, et al. Hepatocyte TAZ/WWTR1 promotes inflammation and fibrosis in nonalcoholic steatohepatitis. Cell Metabol 2016;24(6):848—62.
[51] Xiong X, Wang Q, Wang S, Zhang J, Liu T, Guo L, et al. Mapping the molecular signatures of diet-induced NASH and its regulation by the hepatokine Tsukushi. Mol Metabol 2019;20:128—37.

 © 2024 The Authors. Published by Elsevier GmbH. This is an open access article under the CC BY-NC-ND license (http://creativecommons.org/licenses/by-nc-nd/4.0/).

[52] Flessa CM, Nasiri-Ansari N, Kyrou I, Leca BM, Lianou M, Chatzigeorgiou A, et al. Genetic and diet-induced animal models for non-alcoholic fatty liver disease (NAFLD) research. Int J Mol Sci 2022;23(24).
[53] Gallage S, Avila JEB, Ramadori P, Focaccia E, Rahbari M, Ali A, et al. A researcher's guide to preclinical mouse NASH models. Nat Metab 2022;4(12):1632—49.
[54] Higashi T, Friedman SL, Hoshida Y. Hepatic stellate cells as key target in liver fibrosis. Adv Drug Deliv Rev 2017;121:27—42.
[55] Lai M, Afdhal NH. Liver fibrosis determination. Gastroenterol Clin N Am 2019;48(2):281—9.
[56] Zhang D, Wang S, Ospina E, Shabandri O, Lank D, Akakpo JY, et al. Fructose protects against acetaminophen-induced hepatotoxicity mainly by activating the carbohydrate-response element-binding protein alpha-fibroblast growth factor 21 Axis in mice. Hepatol Commun 2021;5(6):992—1008.
[57] Pozza G, Samardzic N, Giudici F, Casagranda B, N DEM, Palmisano S. Inflammatory-nutritional scores in the diagnosis of NASH and liver fibrosis. Minerva Med 2023;114(1):29—34.
[58] Iroz A, Montagner A, Benhamed F, Levavasseur F, Polizzi A, Anthony E, et al. A specific ChREBP and PPARalpha cross-talk is required for the glucose-mediated FGF21 response. Cell Rep 2017;21(2):403—16.
[59] Pollinger J, Merk D. Therapeutic applications of the versatile fatty acid mimetic WY14643. Expert Opin Ther Pat 2017;27(4):517—25.
[60] Mackenzie LS, Lione L. Harnessing the benefits of PPARbeta/delta agonists. Life Sci 2013;93(25-26):963—7.
[61] Zhu DY, Wu JY, Li H, Yan JP, Guo MY, Wo YB, et al. PPAR-beta facilitating maturation of hepatic-like tissue derived from mouse embryonic stem cells accompanied by mitochondriogenesis and membrane potential retention. J Cell Biochem 2010;109(3):498—508.
[62] Deng Y, Edin ML, Theken KN, Schuck RN, Flake GP, Kannon MA, et al. Endothelial CYP epoxygenase overexpression and soluble epoxide hydrolase disruption attenuate acute vascular inflammatory responses in mice. FASEB J 2011;25(2):703—13.
[63] Zeldin DC. Epoxygenase pathways of arachidonic acid metabolism. J Biol Chem 2001;276(39):36059—62.
[64] Yoshida M, Ishihara T, Isobe Y, Arita M. Genetic deletion of Cyp4f18 disrupts the omega-3 epoxidation pathway and results in psoriasis-like dermatitis. FASEB J 2022;36(12):e22648.
[65] Ford NF. The metabolism of clopidogrel: CYP2C19 is a minor pathway. J Clin Pharmacol 2016;56(12):1474—83.
[66] Hodson L, Gunn PJ. The regulation of hepatic fatty acid synthesis and partitioning: the effect of nutritional state. Nat Rev Endocrinol 2019;15(12):689—700.
[67] Higuchi N, Kato M, Shundo Y, Tajiri H, Tanaka M, Yamashita N, et al. Liver X receptor in cooperation with SREBP-1c is a major lipid synthesis regulator in nonalcoholic fatty liver disease. Hepatol Res 2008;38(11):1122—9.
[68] Benhamed F, Denechaud PD, Lemoine M, Robichon C, Moldes M, Bertrand-Michel J, et al. The lipogenic transcription factor ChREBP dissociates hepatic steatosis from insulin resistance in mice and humans. J Clin Invest 2012;122(6):2176—94.
[69] Sun N, Shen C, Zhang L, Wu X, Yu Y, Yang X, et al. Hepatic Kruppel-like factor 16 (KLF16) targets PPARalpha to improve steatohepatitis and insulin resistance. Gut 2021;70(11):2183—95.
[70] Liang N, Damdimopoulos A, Goni S, Huang Z, Vedin LL, Jakobsson T, et al. Hepatocyte-specific loss of GPS2 in mice reduces non-alcoholic steatohepatitis via activation of PPARalpha. Nat Commun 2019;10(1):1684.
[71] Kang Z, Fan R. PPARalpha and NCOR/SMRT corepressor network in liver metabolic regulation. FASEB J 2020;34(7):8796—809.
[72] Vernia S, Cavanagh-Kyros J, Garcia-Haro L, Sabio G, Barrett T, Jung DY, et al. The PPARalpha-FGF21 hormone axis contributes to metabolic regulation by the hepatic JNK signaling pathway. Cell Metabol 2014;20(3):512—25.
[73] Shi Z, He Z, Wang DW. CYP450 epoxygenase metabolites, epoxyeicosatrienoic acids, as novel anti-inflammatory mediators. Molecules 2022;27(12).
[74] Yao L, Cao B, Cheng Q, Cai W, Ye C, Liang J, et al. Inhibition of soluble epoxide hydrolase ameliorates hyperhomocysteinemia-induced hepatic steatosis by enhancing beta-oxidation of fatty acid in mice. Am J Physiol Gastrointest Liver Physiol 2019;316(4):G527—38.
[75] Wells MA, Vendrov KC, Edin ML, Ferslew BC, Zha W, Nguyen BK, et al. Characterization of the Cytochrome P450 epoxyeicosanoid pathway in non-alcoholic steatohepatitis. Prostaglandins Other Lipid Mediat 2016;125:19—29.
[76] Dhar D, Baglieri J, Kisseleva T, Brenner DA. Mechanisms of liver fibrosis and its role in liver cancer. Exp Biol Med (Maywood) 2020;245(2):96—108.
[77] Kang J, Postigo-Fernandez J, Kim K, Zhu C, Yu J, Meroni M, et al. Notch-mediated hepatocyte MCP-1 secretion causes liver fibrosis. JCI Insight 2023;8(3).
[78] Ihn H. Pathogenesis of fibrosis: role of TGF-beta and CTGF. Curr Opin Rheumatol 2002;14(6):681—5.
[79] Chung SI, Moon H, Ju HL, Cho KJ, Kim DY, Han KH, et al. Hepatic expression of Sonic Hedgehog induces liver fibrosis and promotes hepatocarcinogenesis in a transgenic mouse model. J Hepatol 2016;64(3):618—27.
[80] Inoue M, Jiang Y, Barnes RH, 2nd, Tokunaga M, Martinez-Santibanez G, Geletka L, et al. Thrombospondin 1 mediates high-fat diet-induced muscle fibrosis and insulin resistance in male mice. Endocrinology 2013;154(12):4548—59.

 © 2024 The Authors. Published by Elsevier GmbH. This is an open access article under the CC BY-NC-ND license (http://creativecommons.org/licenses/by-nc-nd/4.0/).